ISSN 1674-1056
http://cpb.iphy.ac.cn
http://iopscience.iop.org/cpb
中国物理 B
Chinese Physics
中国物理 Chinese Physics B

Energy scaling and extended tunability of a ring cavity terahertz parametric oscillator based on $KTiOPO_4$ crystal

Yuye Wang(王与烨), Yuchen Ren(任宇琛), Degang Xu(徐德刚), Longhuang Tang(唐隆煌), Yixin He(贺奕焱), Ci Song(宋词), Linyu Chen(陈霖宇), Changzhao Li(李长昭), Chao Yan(闫超), Jianquan Yao(姚建铨)

Citation: Chin. Phys. B . 2018, 27(11): 114213. **doi:** 10.1088/1674-1056/27/11/114213

Journal homepage: http://cpb.iphy.ac.cn; http://iopscience.iop.org/cpb

What follows is a list of articles you may be interested in

Correction of walk-off-induced wavefront distortion for continuous-wave laser

Hongxin Zou(邹宏新), Guozhu Chen(陈国柱), Yue Wu(伍越), Yong Shen(沈咏), Qu Liu(刘曲)

Chin. Phys. B . 2016, 25(9): 094211. **doi:** 10.1088/1674-1056/25/9/094211

33 W quasi-continuous-wave narrow-band sodium D_{2a} laser by sum-frequency generation in LBO

Wang Peng-Yuan, Xie Shi-Yong, Bo Yong, Wang Bao-Shan, Zuo Jun-Wei, Wang Zhi-Chao, Shen Yu, Zhang Feng-Feng, Wei Kai, Jin Kai, Xu Yi-Ting, Xu Jia-Lin, Peng Qin-Jun, Zhang Jing-Yuan, Lei Wen-Qiang, Cui Da-Fu, Zhang Yu-Dong, Xu Zu-Yan

Chin. Phys. B . 2014, 23(9): 094208. **doi:** 10.1088/1674-1056/23/9/094208

Horizontally slotted photonic crystal nanobeam cavity with embedded active nanopillars for ultrafast direct modulation

Wang Da, Cui Kai-Yu, Feng Xue, Huang Yi-Dong, Li Yong-Zhuo, Liu Fang, Zhang Wei

Chin. Phys. B . 2013, 22(9): 094209. **doi:** 10.1088/1674-1056/22/9/094209

A picosecond widely tunable deep-ultraviolet laser for angle-resolved photoemission spectroscopy

Zhang Feng-Feng, Yang Feng, Zhang Shen-Jin, Xu Zhi, Wang Zhi-Min, Xu Feng-Liang, Peng Qin-Jun, Zhang Jing-Yuan, Wang Xiao-Yang, Chen Chuang-Tian, Xu Zu-Yan

Chin. Phys. B . 2013, 22(6): 064212. **doi:** 10.1088/1674-1056/22/6/064212

Energy scaling and extended tunability of a ring cavity terahertz parametric oscillator based on $KTiOPO_4$ crystal*

Yuye Wang(王与烨)[1,2], Yuchen Ren(任宇琛)[1,2], Degang Xu(徐德刚)[1,2,†], Longhuang Tang(唐隆煌)[1,2], Yixin He(贺奕焱)[1,2], Ci Song(宋词)[3,‡], Linyu Chen(陈霖宇)[1,2], Changzhao Li(李长昭)[1,2], Chao Yan(闫超)[1,2], and Jianquan Yao(姚建铨)[1,2]

[1] *Institute of Laser and Optoelectronics, School of Precision Instruments and Optoelectronic Engineering, Tianjin University, Tianjin* 300072, *China*
[2] *Key Laboratory of Optoelectronic Information Science and Technology (Ministry of Education), Tianjin University, Tianjin* 300072, *China*
[3] *College of Computer and Information Engineering, Tianjin Agricultural University, Tianjin* 300384, *China*

(Received 3 July 2018; revised manuscript received 30 July 2018; published online 25 October 2018)

A wide terahertz tuning range from 0.96 THz to 7.01 THz has been demonstrated based on ring-cavity THz wave parametric oscillator with a $KTiOPO_4$ (KTP) crystal. The tuning range was observed intermittently from 0.96 THz to 1.87 THz, from 3.04 THz to 3.33 THz, from 4.17 THz to 4.48 THz, from 4.78 THz to 4.97 THz, from 5.125 THz to 5.168 THz, from 5.44 THz to 5.97 THz, and from 6.74 THz to 7.01 THz. The dual-Stokes wavelengths resonance phenomena were observed in some certain tuning angle ranges. Through the theoretical analysis of the dispersion curve of the KTP crystal, the intermittent THz wave tuning range and dual-wavelength Stokes waves operation during angle tuning process were explained. The theoretical analysis was in good agreement with the experiment results. The maximum THz output voltage detected by Golay cell was 1.7 V at 5.7 THz under the pump energy of 210 mJ, corresponding to the THz wave output energy of 5.47 μJ and conversion efficiency of 2.6×10^{-5}.

Keywords: terahertz parametric oscillator, $KTiOPO_4$ crystal, extended tunability, energy scaling

PACS: 42.55.Tv, 42.60.By, 42.60.Fc **DOI:** 10.1088/1674-1056/27/11/114213

1. Introduction

Terahertz parametric oscillators (TPOs) based on stimulated polariton scattering have been proven as promising THz wave sources because of their advantages of widely tunable range, high pulse energy, room temperature operation, compactness, coherent radiation, and low cost, which are of great value for various applications such as imaging, molecular analysis, life science, and nondestructive evaluation. The principle of the TPO is the stimulated polariton scattering, which can be sufficiently excited in $LiNbO_3$ (LN), MgO:$LiNbO_3$ (MgO:LN), $KTiOPO_4$ (KTP), $KTiOAsO_4$ (KTA), $RbTiOPO_4$ (RTP), and other crystals.[1–9] Polaritons exhibit both phonon and photon behaviors.[10] Polaritons are the quanta associated with the coupled phonon–photon transverse wave field. The closer the polariton is to the transverse optical (TO) mode of the crystal, the weaker photon characteristic it performs. Over the past few years, numerous research efforts have been made to effectively improve the operation performance of TPOs, such as grating coupling, Si prism coupling, surface emission, injection seeded, pump recycled, and ring cavity configurations.[11–18] These studies were mainly based on MgO:LN crystal with the typical tuning range of 0.6–3.2 THz. Recently, the tuning ranges of TPOs have been broadened with KTP, KTA, and RTP crystals using 1064 nm and 532 nm laser pumping. Especially, the KTP-TPO employing a plane-parallel resonator pumped by 1064 nm laser realized a broadband tuning range of 3.17–6.13 THz, and the maximum THz output of 336 nJ at 5.72 THz.[5] The THz frequency was intermittently tuned from 3.17 THz to 3.44 THz, from 4.19 THz to 5.19 THz, and from 5.55 THz to 6.13 THz, which was simply attributed to the strong absorption of THz wave near the TO mode in KTP crystal in the previous report.

In this work, a KTP-TPO system based on surface-emitted (SE) ring-cavity configuration was demonstrated with a 1064 nm nanosecond pulsed laser pumping. A new wide tuning range from 0.96 THz to 7.01 THz with several gaps was obtained. The maximum terahertz output energy was 5.47 μJ at 5.7 THz under the pump energy of 210 mJ, corresponding to the maximum THz wave conversion efficiency of 2.6×10^{-5}. The widely tunable THz wave was intermittently tuned from 0.96 THz to 1.87 THz, from 3.04 THz to 3.33 THz, from 4.17 THz to 4.48 THz, from 4.78 THz to 4.97 THz, from 5.125 THz to 5.168 THz, from 5.44 THz to 5.97 THz, and from 6.74 THz to 7.01 THz. The dual-Stokes wavelengths resonance phenomena were observed during some tuning angle ranges, corresponding to the two neighboring THz tuning

*Project supported by the National Basic Research Program of China (Grant Nos. 2015CB755403 and 2014CB339802), the National Key Research and Development Program of China (Grant No. 2016YFC0101001), the National Natural Science Foundation of China (Grant Nos. 61775160, 61771332, and 61471257), China Postdoctoral Science Foundation (Grant No. 2016M602954), and Postdoctoral Science Foundation of Chongqing, China (Grant No. Xm2016021).

†Corresponding author. E-mail: xudegang@tju.edu.cn
‡Corresponding author. E-mail: cisong@tjau.edu.cn

© 2018 Chinese Physical Society and IOP Publishing Ltd

ranges. Furthermore, the dispersion curve in THz region for KTP crystal was theoretically analyzed to reveal the characteristics of discontinuities and dual-Stokes wavelengths resonance. The theoretical analysis fitted well with the experiment results. Consequently, this can provide an effective way to explore the output characteristics of KTP in THz region and its isomorphs (KTA, RTP, etc).

2. Experiment setup

A schematic diagram of the KTP-TPO system based on a SE ring-cavity configuration is shown in Fig. 1. The pump source was a multimode Q-switched Nd:YAG laser with the repetition rate of 10 Hz and pulse width of 15 ns. The z-axis polarized pump wave from the Nd:YAG laser was first collimated by the telescope lens T_1, reducing the spot size in order to increase the power density. The combination of the half wave plate (HWP) and Brewster window (BW) was utilized as the attenuator to adjust the energy of the pump wave. An aperture with adjustable diameter, reducing the pump wave diameter to 4 mm, was placed after the telescope lens. M_5 and M_6 were general HR mirrors at the infrared range to adjust the height and incident angle of the pump wave. The ring-cavity was consisted of four mirrors M_1, M_2, M_3, and M_4. The optical arrangement of the cavity was similar to that of the SE ring cavity TPO based on $LiNbO_3$ crystal in our previous report,[15] with some changes of the cavity length due to the different refractive index and cutting angle of KTP crystal. M_1 and M_2 were highly reflective (more than 99%) in the infrared range of 1063–1100 nm for the s-polarization at incident angles of 30° and 65°, respectively. Due to the compact cavity and small phase-matching angle, it is difficult to separate the pump wave and Stokes wave spatially. Specially coating mirrors were fabricated (OCJ/Optical Coatings Japan). M_3 and M_4 were both coated with high transmission (more than 98%) in 1063–1064.7 nm wavelength range and high reflection in the range of 1067–1100 nm ($R > 70\%$@1067–1070 nm, $R > 90\%$@1070–1100 nm) for the s-polarization at the incident angle of 30°. Mirror M_4 was mounted on a high speed optical scanner (Cambridge Technology Inc., 6230H) to rapidly tune the THz wave frequency. It had a maximum angular deflection of ±10° and an excellent scale drift of 50 ppm/°C with the linearity of 99.9% and repeatability of 8 μrad. The response time of the scanner was 600 μs for small angle change of the mirror at the optimum inertia, corresponding to about 600 μs/THz frequency. A faster response time of the scanner than the pulse repetition rate of the pump laser resulted in the fast terahertz frequency tuning from pulse to pulse. The angle was controlled using the output voltage from a computer via a digital-analog converter board (NI, PCIe-6351).

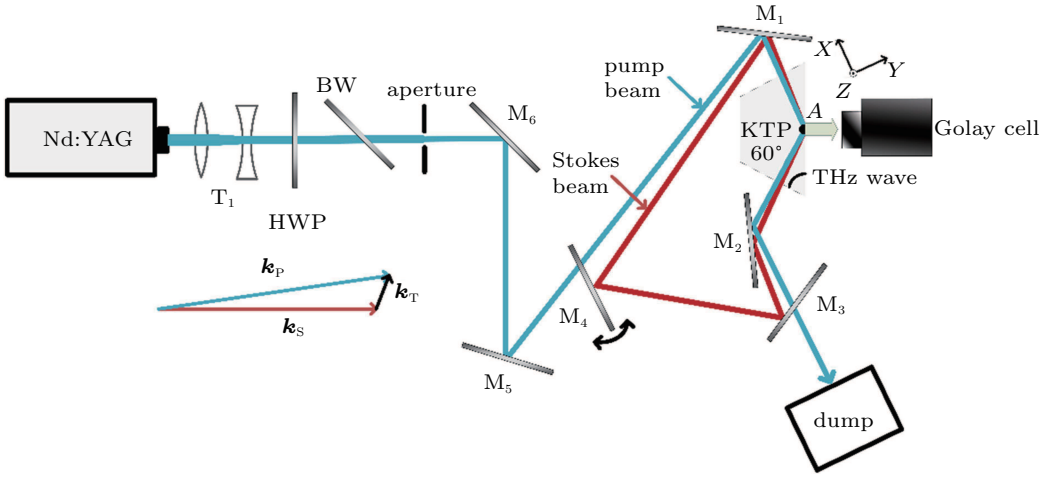


Fig. 1. (color online) Schematic diagram of the experimental setup for the KTP-TPO system based on a SE ring-cavity configuration. The inset shows the noncollinear phase matching condition for THz wave generation in KTP: $\boldsymbol{k}_{\rm p} = \boldsymbol{k}_{\rm S} + \boldsymbol{k}_{\rm T}$.

The nonlinear gain medium was a KTP crystal. The shape of KTP crystal in the x–y plane was an isosceles trapezoid and the waist of incidence was perpendicular to the x-axis of the KTP crystal. The longer base and the shorter base of the isosceles trapezoid are 40 mm and 22 mm, respectively. The thickness of the crystal along the z-axis is 10 mm. The angle between the base and the waist of the isosceles trapezoid is 60°. This kind of design can guarantee that the pump and Stokes waves are totally reflected at the surface, and the THz wave emits perpendicularly to the exit surface of the crystal without any coupler. Point A was assumed to the cross point between the pump and Stokes waves on the totally reflected surface in the KTP crystal, which was fixed when the path of the Stokes light was changed during tuning. The physical cavity lengths for M_1–point A, point A–M_2, M_2–M_3, M_3–M_4, and M_1–M_4 were about 31 mm, 40 mm, 58 mm, 124 mm, and 174 mm, respectively. The incident angle of the pump wave to the crystal surface was fixed at 1.05°, whereas the input voltage to the scanner was linearly varied from 0.21 V to −3.05 V, corresponding to the incident angle of the Stokes light tuning

from 0.63° to −7.15° and the generated THz frequency tuning from 0.96 THz to 7.01 THz. The THz wave output energy was detected by a calibrated Golay cell detector (TYDEX, Inc., GC-1P) at room temperature. The calibration of the Golay cell detector was specified by the manufacturer Tydex to be 92.3 kV/W at a repetition rate of 10 Hz. To block the injection of the intense pump and Stokes pulse into the detector, a transmittance-calibrated black polyethylene sheet (0.75 mm thickness) was used as the THz low-pass filter.

3. Results and discussion

Figure 2 shows the measured THz-wave output energies and Stokes wavelengths of the KTP-TPO system as a function of the optical scanner voltage under the pump energy of 180 mJ. When the voltage of the scanner was changed from 0.21 V to −3.05 V, the detected Stokes light wavelength varied from 1068.16 nm to 1071.9 nm, from 1076 nm to 1077.255 nm, from 1080.52 nm to 1081.72 nm, from 1082.885 nm to 1083.639 nm, from 1084.231 nm to 1084.401 nm, from 1085.499 nm to 1087.677 nm, and from 1090.62 nm to 1091.679 nm. The corresponded THz frequency was from 0.96 THz to 1.87 THz, from 3.04 THz to 3.33 THz, from 4.17 THz to 4.48 THz, from 4.78 THz to 4.97 THz, from 5.125 THz to 5.168 THz, from 5.44 THz to 5.97 THz, and from 6.74 THz to 7.01 THz. The THz output energy in each section of the tuning range appeared in the mountain-shaped curve except the range 1084.231–1084.401 nm due to the narrow range, and it decreased fast near the edge of each section of the tuning range. Furthermore, it should be noticed that dual-Stokes wavelengths appeared when the scanner voltage was from −0.13 V to −0.21 V, and from −0.28 V to −1.36 V, corresponding to the edge regions of four sections of the tuning curve.

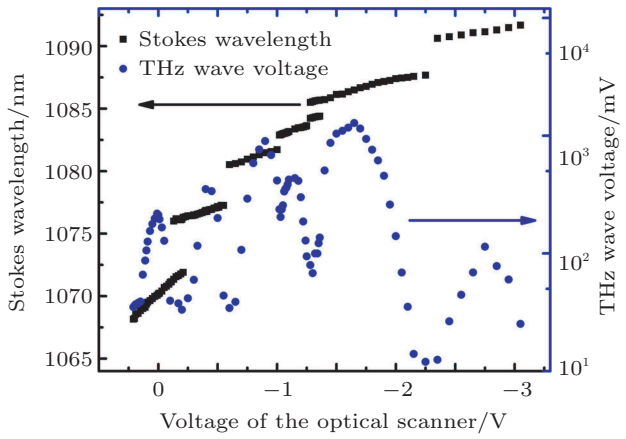


Fig. 2. (color online) Measured THz-wave output energies and Stokes wavelengths of the KTP-TPO system as a function of the voltage of the optical scanner at the pump energy of 180 mJ.

To explore the cause of the output characteristics, including the discontinuities in the Stokes and THz wavelength tuning ranges and dual-Stokes wavelengths, the dispersion characteristics of KTP crystal in the THz region are analyzed in the following part. According to the classical nonlinear phase-matching relationship in TPOs, the energy conservation and momentum conservation should be given as

$$\Omega_{\mathrm{p}} = \Omega_{\mathrm{S}} + \Omega_{\mathrm{T}}, \tag{1}$$

$$|k_{\mathrm{T}}|^2 = |k_{\mathrm{p}}|^2 + |k_{\mathrm{S}}|^2 - 2|k_{\mathrm{p}}||k_{\mathrm{S}}|\cos\theta = (2\pi n_{\mathrm{T}}\Omega_{\mathrm{T}})^2, \tag{2}$$

where Ω_{p}, Ω_{S}, Ω_{T} are the wavenumbers of the pump wave, Stokes wave, and THz wave, respectively, and n_{p}, n_{S}, n_{T} are the refractive indices of the pump wave, Stokes wave, and THz wave in the crystal, respectively. θ is the angle between the pump and the stimulated Stokes waves inside the KTP crystal. The frequency-dependent dielectric constant in the THz region is given by

$$\varepsilon(\Omega) = \varepsilon_\infty + \sum_j S_j \frac{\Omega_{j\mathrm{TO}}^2}{\Omega_{j\mathrm{TO}}^2 - \Omega^2 - \mathrm{i}\Gamma_{j\mathrm{TO}}\Omega}, \tag{3}$$

where $\Omega_{j\mathrm{TO}}$ and $\Gamma_{j\mathrm{TO}}$ are the frequency and the damping coefficient of the j-th TO mode, respectively, S_j is its oscillator strength, and ε_∞ is the high-frequency dielectric constant (subject to certain restrictions, we can regard ε_∞ as the square of the optical refractive index.[10]) The optical refractive index of KTP crystal is from 1.8249 to 1.7381 for the range from 0.4047 μm to 1.064 μm.[19] We use $n_{\mathrm{p}} = 1.7381$ as the optical refractive index in this paper. Additionally, the complex dielectric index for the THz wave in the nonlinear crystal is expressed as

$$\varepsilon(\Omega) = [n(\Omega) + \mathrm{i}\kappa(\Omega)]^2, \tag{4}$$

where the real part $n(\Omega)$ and the imaginary part $\kappa(\Omega)$ are supposed to represent the dispersion and absorption characteristics of the THz wave in the nonlinear crystal, respectively. Furthermore, the absorption coefficient of the THz wave in the nonlinear crystal can be derived as

$$\alpha(\Omega_{\mathrm{T}}) = \frac{2\Omega_{\mathrm{T}}\kappa(\Omega)}{c} = \alpha_{\mathrm{T}}. \tag{5}$$

Thus, based on the parameters of KTP crystal from Ref. [20], the relationship between the phase matching angle and the Stokes wavelength can be calculated in the range of 0–7.65 THz. The result is shown in Fig. 3 (blue line) and it matches well with the experiment results (dotted black line). The small deviation may be related with the parameters of TO modes used in the classical dispersion model. Due to the large number of TO modes with different damping coefficients and oscillator strengths in KTP crystal, there are a lot of spikes on the dispersion curve and it has a great influence on the phase matching process. The most fundamental reason for the THz frequency gap in KTP crystal is that the dielectric constant between the TO and LO modes is purely imaginary. Then, there is no polariton between the TO and LO modes, which makes it

hard to achieve the THz wave output. In the case of the polariton on the dispersion curve between the two neighboring TO modes, the more that it closes to the TO modes, the more mechanical vibration characteristics it performs. Moreover, the polariton processes more mechanical vibration characteristics, influenced by the neighbored TO modes with larger oscillator strength and smaller damping coefficient, which results in no THz wave output and the broadening of the THz frequency gap.

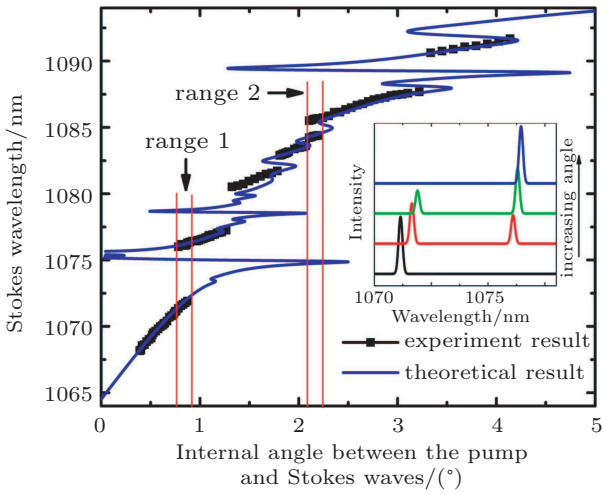


Fig. 3. (color online) Measured (dotted black line) and calculated (blue line) phase matching curves.

The influence of TO modes makes two segments of the dispersion curve exist under some certain phase matching angles. This contributes to the appearance of dual-Stokes wavelengths, indicated as range 1 and range 2 in Fig. 3 in correspondence with tuning angles from 0.78° to 0.87° and from 2.10° to 2.20°. That is to say, there are dual-Stokes wavelengths satisfying the phase matching condition. Hence, the dual-THz wave is expected in these ranges. The inset shows the relative energy change of the dual-Stokes wavelength during the tuning process in range 1. As the angle tuning is performed, the energy of one of the Stokes wavelength is decreased, whereas the energy and wavelength of the other are increased, inducing the neighbored tuning section to begin.

Figure 4 shows the relationship between the calculated absorption for different THz frequencies in KTP crystal and the measured tunable output characteristics of the THz waves from the ring cavity KTP-TPO system at a fixed pump energy of 180 mJ. In range 1 and range 2, there could be dual-frequency THz wave output, so it is difficult to know the exact intensity for the two THz frequencies. To simplify the process, the detected energy of the THz wave in the overlapped range is divided equally for two neighboring tuning ranges. The absorption of the THz wave in KTP crystal is influenced by TO modes and is calculated with Eqs. (3)–(5). On both sides of the peak of the mountain-shaped THz-wave output curves, THz wave energies decreased gradually, which was mainly caused by the strong absorption near the TO modes. The weak energy for the tuning range of 6.74–7.01 THz is the result of the high absorption. The lowest absorption at 6.74 THz in the tuning range 6.74–7.01 THz is 3.71 times larger than the absorption at 5.7 THz, as shown in Fig. 4. It should be mentioned that the THz wave gain is also related with the simulated Raman scattering in KTP crystal. The lower output energy for the tuning range of 0.96–1.87 THz may be attributed to the smaller THz wave gain although the absorption in this range is lower than that at 5.7 THz.

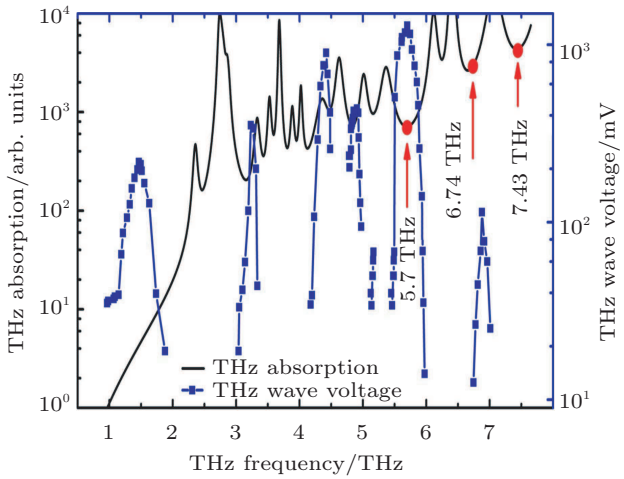


Fig. 4. (color online) The relationship between the absorption for different THz frequencies in KTP crystal and the measured tunable output characteristics of the THz waves from the ring cavity KTP-TPO system at a fixed pump energy of 180 mJ.

Although the higher frequency THz wave could satisfy the phase matching condition in Fig. 3, such as 7.39–7.61 THz (corresponding to the tuning angle of 4.14°–5°), there is no THz output. It can explained as follows. First, the polariton in this range has more mechanical vibration characteristics influenced by the neighbored TO modes with large oscillator strength. Second, the performance of the supermirror is declined and the interaction area among the pump, the Stokes and the THz waves is decreased at larger phase matching angle, which will lead to the lower THz gain. Finally, the THz wave absorption in KTP crystal is very strong in the range of 7.39–7.61 THz with the lowest value at 7.43 THz, which is at least 6.11 times larger than the absorption at 5.7 THz, it also weakens the output of the THz wave.

Figure 5 shows the THz wave output voltage and the conversion efficiency at 5.7 THz as a function of pump energy. The inset shows the THz wavelength measurement by a scanning Fabry–Perot etalon consisted of two parallel THz polarizers, which have a relatively high reflectivity and low absorption at Thz frequency. The THz wave output energy and conversion efficiency increased with the pump energy. The threshold pump energy was 60 mJ. When the pump energy reached 210 mJ/pulse (111.25 MW/cm^2), the detected THz

voltage was 1.7 V and the corresponded THz pulse energy of 5.47 μJ/pulse was achieved, where the maximum light to light conversion efficiency was 2.6×10^{-5} with the pump depletion of 115.5 mJ. Moreover, the corresponding photon conversion efficiency was 0.23%. Higher pump power density was not tried for avoiding the damage to KTP crystal.

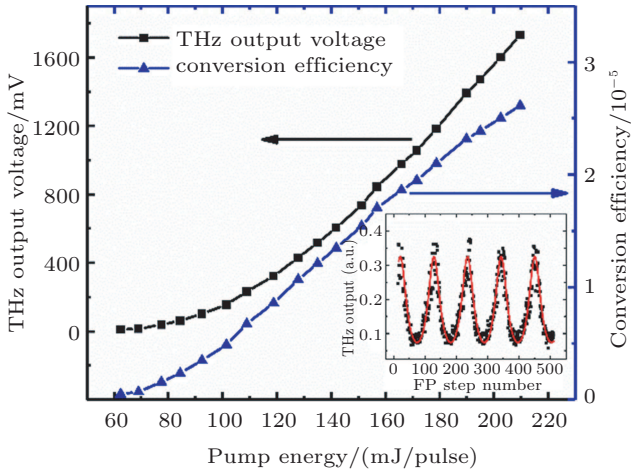


Fig. 5. (color online) THz wave output voltage and light-to-light conversion efficiency under different pump energies at 5.7 THz. The inset shows the THz wavelength measurement by a scanning Fabry–Perot etalon.

4. Conclusion

We have demonstrated a wide tunable and high power THz output based on surface-emitted ring-cavity KTP-TPO. The THz wave was intermittently tuned from 0.96 THz to 1.87 THz, from 3.04 THz to 3.33 THz, from 4.17 THz to 4.48 THz, from 4.78 THz to 4.97 THz, from 5.44 THz to 5.97 THz, and from 6.74 THz to 7.01 THz. The dual-Stokes wavelengths resonance phenomena were observed in some certain tuning angle ranges. A theoretical analysis of the dispersion curve in KTP crystal was given to reveal the characteristics of the intermittently tuned range and dual-Stokes wavelengths resonance. This is in good agreement with the experiment results. The maximum THz output voltage detected by Golay cell was 1.7 V at 5.7 THz under the pump energy of 210 mJ, corresponding to the THz energy of 5.47 μJ and conversion efficiency of 2.6×10^{-5}.

References

[1] Johnson B C, Puthoff H E, SooHoo J and Sussman S S 1971 *Appl. Phys. Lett.* **18** 181
[2] Pasiskevicius V, Canalias C and Laurell F 2006 *Appl. Phys. Lett.* **88** 41110
[3] Piestrup M A, Fleming R N and Pantell R H 1975 *Appl. Phys. Lett.* **26** 418
[4] Wang W, Cong Z, Liu Z, Zhang X, Qin Z, Tang G, Li N, Zhang Y and Lu Q 2014 *Opt. Express* **22** 17092
[5] Wang W, Cong Z, Chen X, Zhang X, Qin Z, Tang G, Li N, Wang C and Lu Q 2014 *Opt. Lett.* **39** 3706
[6] Yan C, Wang Y, Xu D, Xu W, Liu P, Yan D, Duan P, Zhong K, Shi W and Yao J 2016 *Appl. Phys. Lett.* **108** 011107
[7] Yarborough J M, Sussman S S, Purhoff H E, Pantell R H and Johnson B C 1969 *Appl. Phys. Lett.* **15** 102
[8] Ortega T A, Pask H M, Spence D J and Lee A J 2016 *Opt. Express* **24** 10254
[9] Li Z Y, Yao J Q, Li J, Bing P B, Xu D G and Wang P 2010 *Acta Phys. Sin.* **59** 6237 (in Chinese)
[10] Yurii N P 1978 *Soviet Physics Uspekhi* **21** 805
[11] Kawase K, Sato M, Taniuchi T and Ito H 1996 *Appl. Phys. Lett.* **68** 2483
[12] Ikari T, Zhang X, Minamide H and Ito H 2006 *Opt. Express* **14** 1604
[13] Tonouchi M 2007 *Nat. Photon.* **1** 97
[14] Minamide H, Ikari T and Ito H 2009 *Rev. Sci. Instrum.* **80** 123104
[15] Yang Z, Wang Y, Xu D, Xu W, Duan P, Yan C, Tang L and Yao J 2016 *Opt. Lett.* **41** 2262
[16] Wu D H and Ikari T 2009 *Appl. Phys. Lett.* **95** 141105
[17] Xu D G, Zhang H, Jiang H, Wang Y Y, Liu C M, Yu H, Li Z Y, Shi W and Yao J Q 2013 *Chin. Phys. Lett.* **30** 024212
[18] Imai K, Kawase K, Shikata J, Minamide H and Ito H 2001 *Appl. Phys. Lett.* **78** 1026
[19] Fan T Y, Huang C E, Hu B Q, Eckardt R C, Fan Y X, Byer R L and Feigelson R S 1987 *Appl. Opt.* **26** 2390
[20] Kugel G E, Brehat F, Wyncke B, Fontana M D, Marnier G, Carabatos-Nedelec C and Mangin J 1988 *J. Phys. C: Solid State Phys.* **21** 5565